

The Deuterium Abundance at $z=0.701$ towards QSO 1718+4807¹

David Tytler², Scott Burles³, Limin Lu, Xiao-Ming Fan, Arthur Wolfe
 Department of Physics, and Center for Astrophysics and Space Sciences
 University of California, San Diego
 C0424, La Jolla, CA 92093-0424

Blair D. Savage
 Washburn Observatory
 University of Wisconsin
 475 N. Charter Street
 Madison, WI 53706

ABSTRACT

We present constraints on the deuterium to hydrogen ratio (D/H) in the metal-poor gas cloud at redshift $z = 0.701$ towards QSO 1718+4807. We use new Keck spectra in addition to Hubble Space Telescope (HST) and International Ultraviolet Explorer (IUE) spectra. We use an improved redshift and a lower H I column density to model the absorption. The HST spectrum shows an asymmetric Lyman- α ($\text{Ly}\alpha$) feature which is produced by either H I at a second velocity, or a high abundance of D. Three models with a single simple H+D component give $8 \times 10^{-5} < \text{D}/\text{H} < 57 \times 10^{-5}$ (95%), a much larger range than reported by Webb *et al.* (1997a,b). A more sophisticated velocity distribution, or a second component is necessary for lower D/H. With two components, which could be a part of one absorbing structure, or separate clouds in a galaxy halo, we find $\text{D}/\text{H} < 50 \times 10^{-5}$. We do not know if this second component is present, but it is reasonable because 40 – 100% of absorption systems with similar redshifts and H I column densities have more than one component.

Subject headings: quasars: absorption lines — quasars: individual (Q1718+4807)

¹Based on observations obtained with the NASA/ESA Hubble Space Telescope obtained by the Space Telescope Science Institute, which is operated by AURA, Inc., under NASA contract NAS5-26555.

²Visiting Astronomer, W. M. Keck Telescope, California Association for Research in Astronomy

³Present address: University of Chicago, Dept. of Astronomy & Astrophysics, 5640 S. Ellis Ave., Chicago, IL 60637

1. INTRODUCTION

The absorption system at $z = 0.701$ towards Q1718+4807 is well suited for a determination of D/H from analysis of the line profiles of the Lyman series. We selected this line of sight to measure D/H for four reasons: (1) Low redshift Lyman lines are likely to be less contaminated by unrelated H I Ly α lines. (2) The background QSO is bright and affords the possibility of high resolution UV spectroscopy with HST. (3) IUE spectra of the QSO (Lanzetta, Turnshek, & Sandoval 1993) show a partial Lyman limit which is very steep, which implies that the Lyman series lines are unusually narrow. At high redshift most Lyman lines are broad enough that they swallow the D lines. (4) Metal lines in Keck optical spectra were very weak. We now estimate that HST+FOS spectra limit the system’s metallicity to less than 1/100 solar.

Webb *et al.* (1997a, 1997b, hereafter WCLFLV) have studied this system in detail and find $D/H = 20 \pm 5 \times 10^{-5}$. They assume the absorber is simple, with a single velocity component (e.g. one cloud in a halo) and they assume that it produces lines with Voigt profiles. These assumptions are justified by the simple appearance of the Si III and Mg II lines and the steep Lyman Limit, but they are ruled out by the asymmetric Ly α line, unless D/H is very high.

Levshakov *et al.* (1998) use the same data as WCLFLV and apply more sophisticated models which allow for correlations in the velocity field (non-Voigt profiles). They use realistic parameters for the gas: temperatures from $1.4 - 1.8 \times 10^4$ K, and turbulent velocities of $18 - 40$ km s $^{-1}$. Their models produce asymmetric profiles for the H I Ly α absorption, with more H I absorption and less D on the blue side of the Ly α line, and they find a lower estimate of $D/H \simeq 4.4 \times 10^{-5}$. These models allow only one velocity component, and they assume that both the temperature and RMS turbulent velocity are constant along the line of sight through this absorber.

In this letter, we present new Keck spectra, and analyze the range of D/H allowed by the HST+GHRS, HST+FOS, and IUE spectra for this absorber. In Section 2, we describe the spectroscopic observations and results from the four different instruments. In Section 3, we investigate a set of four models to analyze the systematic differences in the derived D/H between models. We also assess the magnitudes of other possible systematic effects.

2. OBSERVATIONS & ANALYSIS

On March 3, 1995, the observations of QSO 1718+4807 ($z_{em} = 1.084$, $V = 15.3$) were obtained with the GHRS on HST. Fifty-six five minute exposures of QSO 1718+4807, each covering 2050–2099 Å were taken with the G270M grating. We used the small science aperture (SSA) to reduce the blurring effects of the HST spherical aberration in these post-COSTAR observations. COSTAR refers to the corrective optical system installed in the HST during the 1993 December Space Shuttle repair mission. We observed the QSO in the FP-SPLIT= 4 sequence to reduce the effects of detector/photocathode fixed pattern noise. Detector scanning step pattern

number 4 provided two samples per diode width and sampling of the object spectrum and the detector background with the full 500 channel array of the GHRS Digicon detector. We spent 11% of the observing time on the background observations. For technical descriptions of the GHRS, see the Space Telescope Science Institute Instrument Handbooks (Solderblom *et al.* 1994).

We processed the data with the HST CALHRS reduction system developed by the GHRS science team. The data reduction converts raw counts into count rates, adjusting for pulse counting dead time losses, particle radiation, dark count events and diode to diode sensitivity variations. Because of the low signal level in the individual spectra, we used a standard merge to combine the fifty-six integrations into a single spectrum. The line spread function (LSF) for these SSA observations should be well represented by a Gaussian with $\text{FWHM} = 14 \text{ km s}^{-1}$ (Gilliland *et al.* 1992; Robinson *et al.* 1998), which is consistent with the profile width we measured for wavelength calibration arc lamp observations obtained before and after the object integrations.

In this analysis, we use the wavelength scale given by WAVECAL exposures which we obtained during the GHRS observations of QSO 1718+4807, and we use the reduction package written by the GHRS team. We find a wavelength offset of 16.4 km s^{-1} from the spectrum analyzed by WCLFLV, the difference most likely arising in an offset between the default GHRS wavelength scale and the wavelength calibrations taken between science exposures. The WAVECAL calibrations gives a more accurate scale for the GHRS spectrum and we use this scale throughout the paper. The spectrum is shown in Figure 1, along with a cubic spline which we use to fit the quasar continuum.

At the redshift of interest, $z = 0.7011$, two absorption lines are seen in the GHRS spectrum: $\text{Ly}\alpha$ and Si III. The diodes are 0.098 \AA wide (or 14.2 km s^{-1}) and two samples were taken per diode width. The signal-to-noise ratio (SNR) is approximately 9 per diode sample. The Si III($\lambda 1206$) line is best fit with a single Voigt profile at $z = 0.701117 \pm 0.000008$ with a column density, $\log N(\text{Si III}) = 12.85 \pm 0.05 \text{ cm}^{-2}$, and velocity dispersion, $b = 17 \pm 2 \text{ km s}^{-1}$ ($b = \sqrt{2}\sigma$). The column density and velocity dispersion for Si III measured in our GHRS spectrum agree with WCLFLV, but the measured redshift is offset by 16.4 km s^{-1} due to the different wavelength calibrations.

We obtained optical spectra of QSO 1718+4807 with the HIRES spectrograph (Vogt *et al.* 1994) on the 10-m Keck-1 telescope, with spectral resolution of 8 km s^{-1} (FWHM) and full wavelength coverage from 3800 \AA to 5000 \AA . We performed a standard spectral extraction, described by Tytler, Fan & Burles (1996). Three exposures totalling 4500 seconds gave $\text{SNR} = 50$ per 2 km s^{-1} pixel at the wavelengths of Mg II. As is common with most QSO metal-line systems, we detected Mg II ($\lambda\lambda 2796, 2803$), but not Fe II ($\lambda\lambda 2344, 2382, 2600$). We measure $\log N(\text{Mg II}) = 11.5 \pm 0.1 \text{ cm}^{-2}$, $z(\text{Mg II}) = 0.701088 \pm 0.000007$, $b(\text{Mg II}) = 13.5 \pm 1.9 \text{ km s}^{-1}$, and place an upper limit for the Fe II column density of $\log N(\text{Fe II}) < 12.6 \text{ cm}^{-2}$.

Figure 2 shows the useful absorption lines at redshift $z = 0.7011$. The three metal lines, Si III ($\lambda 1206$) and Mg II ($\lambda\lambda 2796, 2803$) are optically thin and best fit with single Voigt profiles. The velocity difference between the Si III and Mg II lines is $5.1 \pm 1.9 \text{ km s}^{-1}$, where this 1σ error

ignores errors in the wavelength scales. This difference is most likely due to the external error on the GHRS wavelength scale from the WAVECAL exposures, which has an RMS of $\Delta v = 3.5$ km s⁻¹ and a maximum of $\Delta v = 10$ km s⁻¹, and hence the Si III and Mg II may arise in the same gas.

The neutral hydrogen column density is well constrained by the Lyman limit which has optical depth near unity (Lanzetta, Turnshek, & Sandoval 1993), and is responsible for the continuous absorption below 1550 Å in the IUE spectrum (Figure 3). We estimate the column density and 1σ errors $\log N(\text{H I}) = 17.12 \pm 0.05$ cm⁻². The error in $N(\text{H I})$ is much smaller than the final error in D/H. Another hydrogen system at $z = 0.602$ also contributes to the optical depth below 1460 Å, with $\log N(\text{H I}) \simeq 16.7$ cm⁻². WCLFLV fit the quasar continuum below 1550 Å with just the system at $z = 0.701$, and found $\log N(\text{H I}) = 17.24 \pm 0.01$ cm⁻². We suggest this column density is too high, because the lower redshift Lyman limit system accounts for some of the absorption below 1460 Å.

We can estimate the temperature, metallicity, and neutral fraction in this absorption system. We use velocity information available for H I and Mg II to convert equivalent widths of other ions into approximate column densities. The velocity dispersions are well constrained for H I and Mg II by fitting single Voigt profiles. For these two low-ionization species the observed columns may, but need not, come from the same gas. If we assume the temperature and turbulent velocity is identical for both species, we find $T = 3.1 \pm 0.5 \times 10^4$ K and $b_{tur} = 12.7 \pm 2.0$ km s⁻¹.

In archived spectra obtained with the HST Faint Object Spectrograph ($R \approx 1300$ – too small to give column densities), we measure equivalent widths $W_{obs}(\text{C IV}) = 0.13, 0.09$ Å for the C IV ($\lambda\lambda 1548, 1550$) doublet at $z = 0.701$. Using the above values for T and b_{tur} , this implies a column density $\log N(\text{C IV}) = 13.3 \pm 0.2$ cm⁻². We place an upper limit on the column density of Si II using a 2σ upper limit on the equivalent width of Si II ($\lambda 1260$), $\log N(\text{Si II}) < 12.3$ cm⁻². We estimated the metal abundance using the photoionization code CLOUDY (Ferland 1993). We used an ionizing background spectrum at $z = 0.7$ from Haardt & Madau (1997), and we assumed that the ratio of the two alpha elements Mg and Si is solar. We find unremarkable parameters: an ionization parameter $\log U = -2.5$, a total hydrogen density $n_H = 10^{-3.1}$ cm⁻², and a neutral fraction of $n(\text{H I})/n_H = 10^{-2.9}$, and a low metal abundance $[\text{Si}/\text{H}] = -2.4$.

3. Constraining D/H

We measure D/H by comparing composite Voigt profile models with the QSO spectra. We consider four models which differ in the number of Voigt profiles used, and other constraints. In each model, we adjust the parameters to minimize the χ^2 . The value of D/H depends varies a lot depending on the redshift(s) assumed for the H. This should be measured from the high order Lyman series lines, which will be much less saturated than Ly α , and hence will hence show more details of the velocity distribution. Since this data has not been obtained, we use the redshifts

of the metal lines as constraints in Models 1 and 2. In Table 1, we list the assumed redshift in each model. All models except 4 have a single velocity component, which produces a blend of H I and D I lines. In Model 3 we leave the redshift of the H free. In Model 4, we allow H at a second redshift which absorbs flux near $z(\text{D I})$. We do not use metal lines to constrain the velocity dispersion and temperature of the H and D because this would be an unnecessary constraint, which could be inaccurate, e.g. if variations in the ionization and metallicity give different parameters for the H and metals.

For each model we step through values of D/H, $-5.0 < \log(\text{D}/\text{H}) < -3.0$ and fit to the GHRS data between $2066 \text{ \AA} < \lambda < 2070 \text{ \AA}$, with a constraint on N(H I) measured with the Lyman limit. We perform a least squares minimization of all free parameters in the models over a range of D/H (Burles & Tytler 1998). This gives a measure of χ^2 as a function of the single parameter D/H. We calculate the most likely D/H and confidence levels from the χ^2 functions (Figure 4). In table 1, we list the minimum χ^2_{min} , the corresponding value of D/H with 95% confidence levels, and the χ^2 probability that the data came from the model.

In Table 2 we show that other uncertainties in the measurement are much smaller than the differences in the models and the random errors, with the exception of the one-sided uncertainty due to contaminating absorption. We estimate the uncertainty as $\Delta \log \left(\frac{\text{D}}{\text{H}} \right) = -\log \left(1 - \frac{\text{N}(\text{C})}{\text{N}(\text{D I})} \right) \ln(1 - \text{P})$, where P is the probability of contamination by an absorber with column density N(C). With the above estimates from Mg II systems, this uncertainty can be as high as $\Delta \log(\text{D}/\text{H}) \approx 1$.

The unabsorbed intrinsic quasar continuum level is well determined: an error of 5% would give $\Delta \log \text{D}/\text{H} < 0.04$ in all models. The H I and D I lines have FWHMs greater than 41 km s^{-1} and 36 km s^{-1} respectively and the D/H is not sensitive to changes in the line spread function, which calibration spectra show is a Gaussian with $\text{FWHM} = 14 \text{ km s}^{-1}$.

3.1. Is there a Second Component to H?

There are two possible origins for the second hydrogen component: the random Ly α forest and gas associated with the D/H system. We discuss the likelihood of each. The low column density Ly α forest has not yet been measured at these redshifts, but we can estimate the line density directly from the GHRS spectrum in Figure 1. Assuming that the four unidentified lines are H I Ly α lines, we estimate a line density $\frac{dN}{dz} \simeq 166$ for Ly α lines with column densities $12.5 \text{ cm}^{-2} < \text{Log N}(\text{H I}) < 14.5 \text{ cm}^{-2}$ for $z = 0.7$. We calculate the probability of one or more Ly α lines to fall within 20 km s^{-1} of the expected D I position, $\text{P} \simeq 1\%$. This probability is calculated after the inspection of the data (*a posteriori*). Chance events often give much lower values for such probabilities.

We know less about the velocity structure of low column, low redshift Lyman limit systems. We would like to know, given that an LLS has been seen, what is the probability that it has

only one velocity component in H I? There is no relevant data on H I, but Keck telescope HIRES spectra provide clues. Charlton & Churchill (1998) found that all Mg II systems in a sample of 26 at low redshift ($z < 1$) show 2 or more components in Mg II. This sample was restricted to Mg II lines with $W_r(2796) > 0.3 \text{ \AA}$ and would not have contained our Mg II line, which is unusually weak with $W_r(2796) = 0.013 \text{ \AA}$.

A second sample of Mg II lines with $0.02 < W_r < 0.3 \text{ \AA}$ was presented by Churchill *et al.* (1998). The redshift range is appropriate: 0.4 – 1.2, peaking near 0.7. About 40% of these 30 systems have more than one component or show wide lines indicative of velocity structure. There are three reasons why the relevant fraction is $> 40 \%$. 1. Many of their spectra are of low SNR and would not show weak Mg II components. 2. H I is often seen in gas where Mg II is not detected in even the highest current SNR spectra. 3. From the number of lines per unit redshift, they calculate that 74% of their systems do not have enough H I to show Lyman breaks, and hence they have less H I than the absorber in 1718+4807. Clustering increases with H I column (Cristiani *et al.* 1997), and hence we expect that the sub-sample with larger N(H I), comparable to the 1718 absorber, will show more components. On the other hand, 1718 has extremely weak Mg II lines and it was selected because the LLS seemed unusually steep in IUE spectra, which should exclude the more complex systems, and decrease the probability that 1718 would show more than one component. In summary, the probability that an absorber with H I column like that in 1718+4807 shows more than one component is in the range 40 – 100%. The probability that the absorber in 1718 has more than one component will be lower than this, because we know its LLS is steep, the Mg II lines are weak, and they and the Si III line are simple, but we do not use this information because it would give an *a posteriori* probability, which would be hard to interpret.

4. SUMMARY

This is the first QSO absorption system to give limits on D/H at a moderate redshift. Compared to other systems at $z > 2.5$, this D/H limit is less reliable because the low signal to noise in the Ly α line and the lack of spectra of other Lyman series lines allow a variety of models which give a wide range of possible D/H. The reduced contamination by the random Ly α forest is an advantage which does not compensate for the other two disadvantages.

Four lines are detected in high resolution spectra. Si III and Mg II show simple lines which can come from a simple model with one velocity component which gives Voigt line profiles. In this case the asymmetry of the Ly α line must be explained by another ion. The wavelength of the asymmetric absorption is a good match to the expected location of D. Our three models of this situation use different assumptions about the redshift of the gas and give 95% confidence levels in the range $8 \times 10^{-5} < D/H < 57 \times 10^{-5}$.

The asymmetric Ly α line can equally well be modeled with a more sophisticated velocity distribution. Levshakov *et al.* (1998) found models which give $D/H \simeq 4.4 \times 10^{-5}$ if there are

significant correlations in the velocity field. We present a model with gas at two velocities which gives the upper limit $D/H < 50 \times 10^{-5}$. Absorbers with similar H I columns show complex velocity structure in 40 – 100% of cases. The probability that this absorber is complex will be lower because we know that the Si III and Mg II lines appear simple, and the Lyman limit is steep. The dominant uncertainty in the D/H comes from our ignorance of the H I velocity field. If it is simple then the uncertainty in the redshift of this component, and random errors from the low signal to noise each give about a factor of two uncertainty (95%) in D/H.

We find a good fit to the metal lines using a solar Mg/Si abundance ratio, and $[Si/H] = -2.4 \pm 0.1$. Even though the system is at a much lower redshift than previous D/H observations, the low metallicity suggests minimal chemical processing.

A high value of D/H ($> 10^{-4}$) gives a low cosmic baryon density, $\Omega_b < 0.01h^{-2}$, where $H_0 = 100 h \text{ km s}^{-1}$. In standard big bang nucleosynthesis, a value for D/H fixes the cosmological baryon to photon ratio and predicts the primordial abundances of other elements. The high D/H is consistent with some estimates of the primordial ^4He abundance (Pagel *et al.* 1992, Olive & Steigman 1995, Olive *et al.* 1997), but not others (Izotov and Thuan 1998). The high D/H is not consistent with galactic chemical evolution (Tosi *et al.* 1998) or with other independent measures of Ω_b , from the Lyman- α forest (Bi & Davidsen 1997, Rauch *et al.* 1997, Weinberg *et al.* 1997, Zhang *et al.* 1998), galaxy clusters (Schramm 1998), and early data on the power spectrum of the cosmic microwave background (Lineweaver & Barbosa 1998).

Two other QSOs give low values of $D/H = 3.4 \pm 0.3 \times 10^{-5}$ (Burles & Tytler 1998a,b) which is consistent with all other QSO data, but not with the high D/H. Low D/H implies a high baryon density consistent with other measures. Clearly, new measures of D/H in other QSOs are urgently needed.

This work was funded in part by a grant from the Space Telescope Science Institute, GO-5488 and by G-NASA/NAG5-3237. We are grateful to Steve Vogt, the PI of the Keck HIRES instrument, and Theresa Chelminiak, Barbara Schaefer who assisted us in obtaining the Keck spectra. We thank the anonymous referee whose insight and support improved the manuscript.

REFERENCES

- Bi, H. & Davidsen, A. F. 1997, ApJ, 479, 523
Burles, S. & Tytler, D. 1998, ApJ, 499, 699
Burles, S. & Tytler, D. 1998, ApJ, 507, in press
Churchill, C.W., Rigby, J.R., Charlton, J.C. & Vogt, S. 1998, ApJ, in press
Charlton, J. C. & Churchill, C. W. 1998, ApJ, 499, 181

- Cristiani, S., D'Odorico, S., D'Odorico, V., Fontana, A., Giallongo, E., & Savaglio, S. 1997, MNRAS, 285, 209
- Ferland, G. 1993, Univ. Kentucky Dept. Physics and Astron. Internal Rept.
- Gilliland, R. L., Morris, S. L., Weymann, R. J., Ebbets, D. C., & Lindler, D. J. 1992, PASP, 104, 367
- Haardt, F. & Madau, P. 1997, ApJ, 461, 20
- Lanzetta, K. M., Turnshek, D. A., & Sandoval, J. 1993, ApJS, 84, 109
- Levshakov, S.A., Kegel, W.H. & Takahara, F. 1998, A & A, 336, L29
- Lineweaver, C. H. & Barbosa, D. 1998, ApJ, 498, 624
- Olive, K. A. & Steigman, G. 1995, ApJS, 97, 49
- Olive, K. A., Skillman, E. D., & Steigman, G. 1997, ApJ, 483, 788
- Pagel, B. E. J., Simonson, E. A., Terlevich, R. J. & Edmunds, M. G. 1992, MNRAS, 255, 325
- Rauch, M., Miralda-Escude, J., Sargent, W. L. W., Barlow, T. A., Weinberg, D. H., Hernquist, L., Katz, N., Cen, R., & Ostriker, J. P. 1997, ApJ, 489, 7
- Robinson, R.D. *et al.* 1998, PASP, 110, 68
- Schramm, D. 1998, in Primordial Nuclei and their Galactic Evolution, eds. N. Prantzos, M. Tosi, & R. von Steiger (Kluwer, Dodrecht), 3
- Solderblom, D.R., Hulbert, S.M., Leither, C., & Sherbert, L.E., 1994, Goddard High Resolution Spectrograph Instrument Handbook, v5 (Space Telescope Science Institute, Baltimore)
- Tosi, M., Steigman, G., Matteucci, F., & Chiappini, C. 1998, ApJ, 498, 226
- Tytler, D., Fan, X-M., & Burles S. 1996, Nature, 381, 207
- Vogt, S. S., *et al.* 1994, Proc. SPIE, 2198, 362
- Webb, J. K., Carswell, R. F., Lanzetta, K. M., Ferlet, R., Lemoine, M., Vidal-Madjar, A., & Bowen, D. V. 1997a, Nature, 388, 250
- Webb, J. K., Carswell, R. F., Lanzetta, K. M., Ferlet, R., Lemoine, M., & Vidal-Madjar, A. 1997b, preprint, astro-ph 9710089, (WCLFLV)
- Weinberg, D. H., Miralda-Escude, J., Hernquist, L., & Katz, N. 1997, ApJ, 490, 564
- Zhang, Y., Meiksin, A., Anninos, P., Norman, M. L. 1998, ApJ, 495, 63

D/H Absorption Models

Model	Redshifts	χ_{min}^2	D/H (-2σ) ^a	D/H(χ_{min}^2) ^a	D/H ($+2\sigma$) ^a	par ^b	P(χ_{min}^2) ^c
1	$z_1 = z(\text{Si III})$	44.8	-3.78	-3.60	-3.44	4	0.37
2	$z_1 = z(\text{Mg II})$	51.2	-4.08	-3.86	-3.62	4	0.25
3	z_1 free	43.7	-3.80	-3.46	-3.24	5	0.37
4	z_1, z_2 both free	42.0	... ^d	...	-3.30	8	0.30

^aIn logarithmic units

^bNumber of free parameters in model

^cFit with 46 diode samples in GHRS spectrum covering Ly α

^dLower limit extends to below parameter range of $\log(\text{D}/\text{H}) = -5.0$

Uncertainties in the D/H measurement^a

Uncertainty	Magnitude ^b
Choice of Model	± 0.40
Random Errors	± 0.34 ^c
Total Hydrogen ^d	± 0.10
Continuum Placement	± 0.04
Line Spread Function	± 0.02
Interloping Hydrogen	$\approx -1.0 \times P_i$ ^e

^aCorresponding to 95% confidence

^bIn logarithmic units of $\log \text{D}/\text{H}$

^cLargest 95% uncertainty error in Table 1

^dEstimated from Lyman continuum absorption

^eDepends on the probability of interloper, P_i

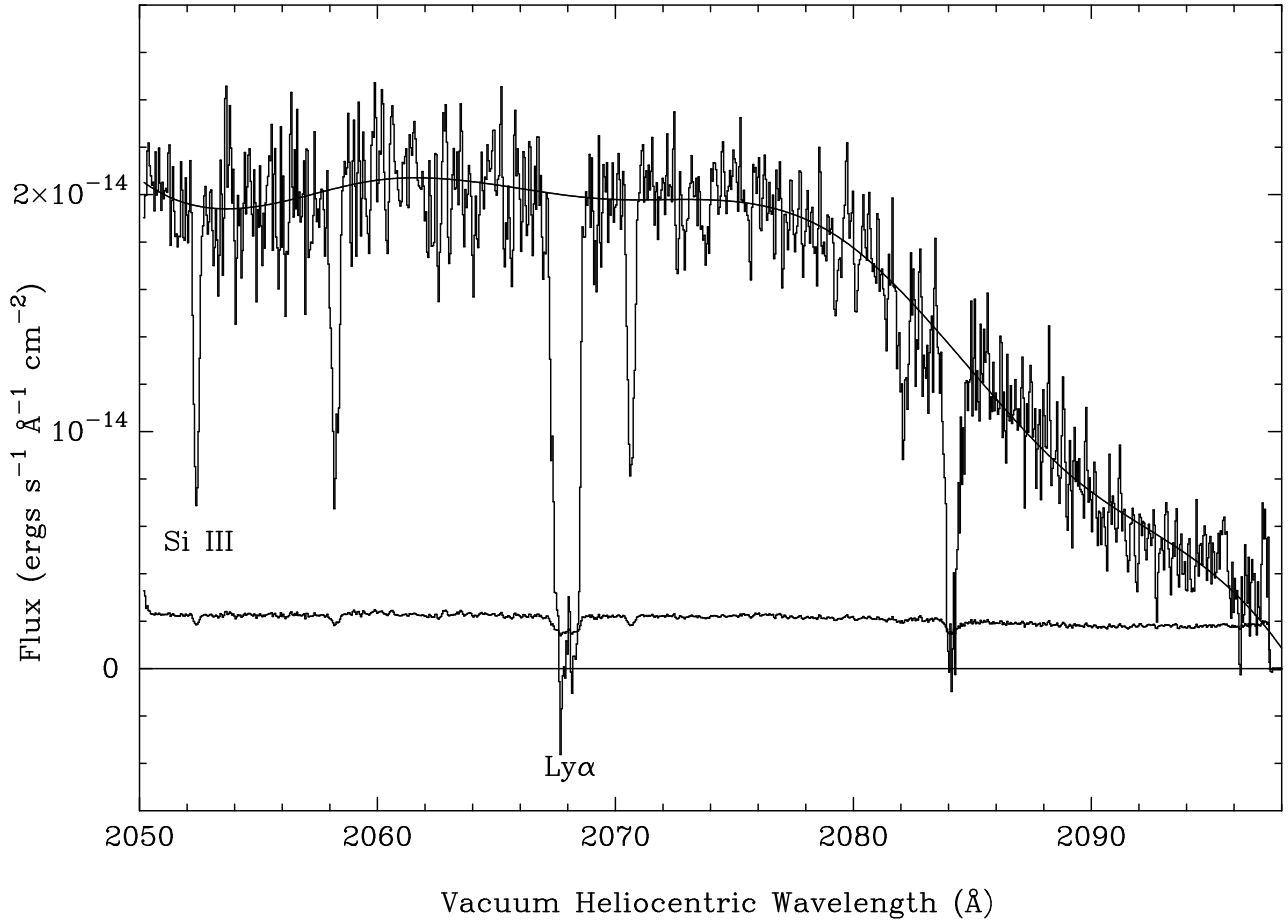


Fig. 1.— GHRM spectrum of QSO 1718+4807. The histogram shows the observed flux, the lower line is the 1σ error per diode sample, and the solid line is the continuum fit. The spectrum was obtained with 14.2 km s^{-1} wide diodes with two samples per diode width. The Ly α feature of interest is seen at 2068 \AA , and the corresponding Si III line is at 2052 \AA . The SNR is 9 per diode sample at Ly α and Si III.

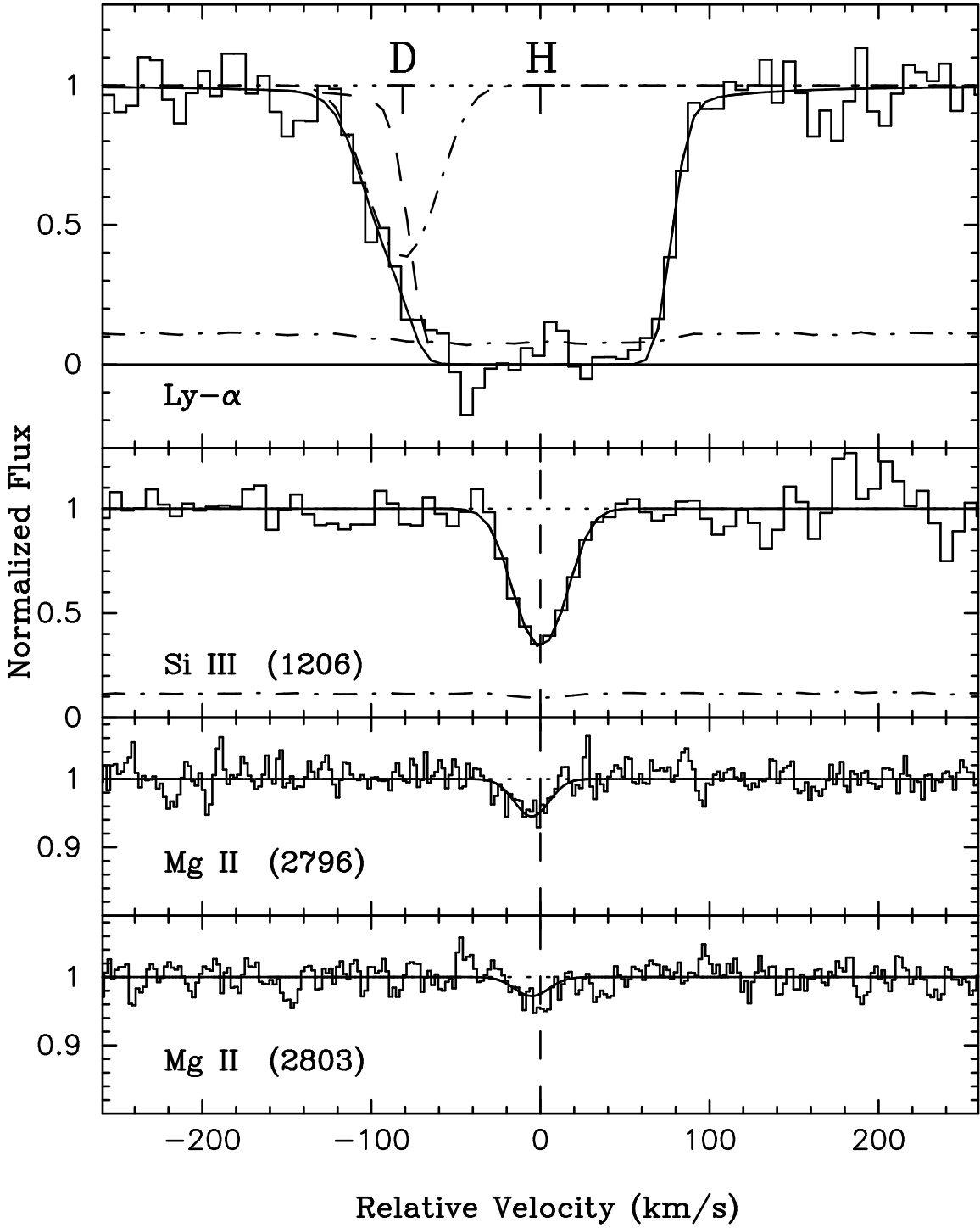


Fig. 2.— Velocity plots of Lyman α , Si III (1206), and Mg II (2796,2803) absorption features in the system towards QSO 1718+4807. Zero velocity corresponds to the redshift $z = 0.701117$ measured for Si III. The histogram represents the observed counts in each diode sample normalized to the quasar continuum. The smooth line shows a typical composite Voigt profile fit to the data.

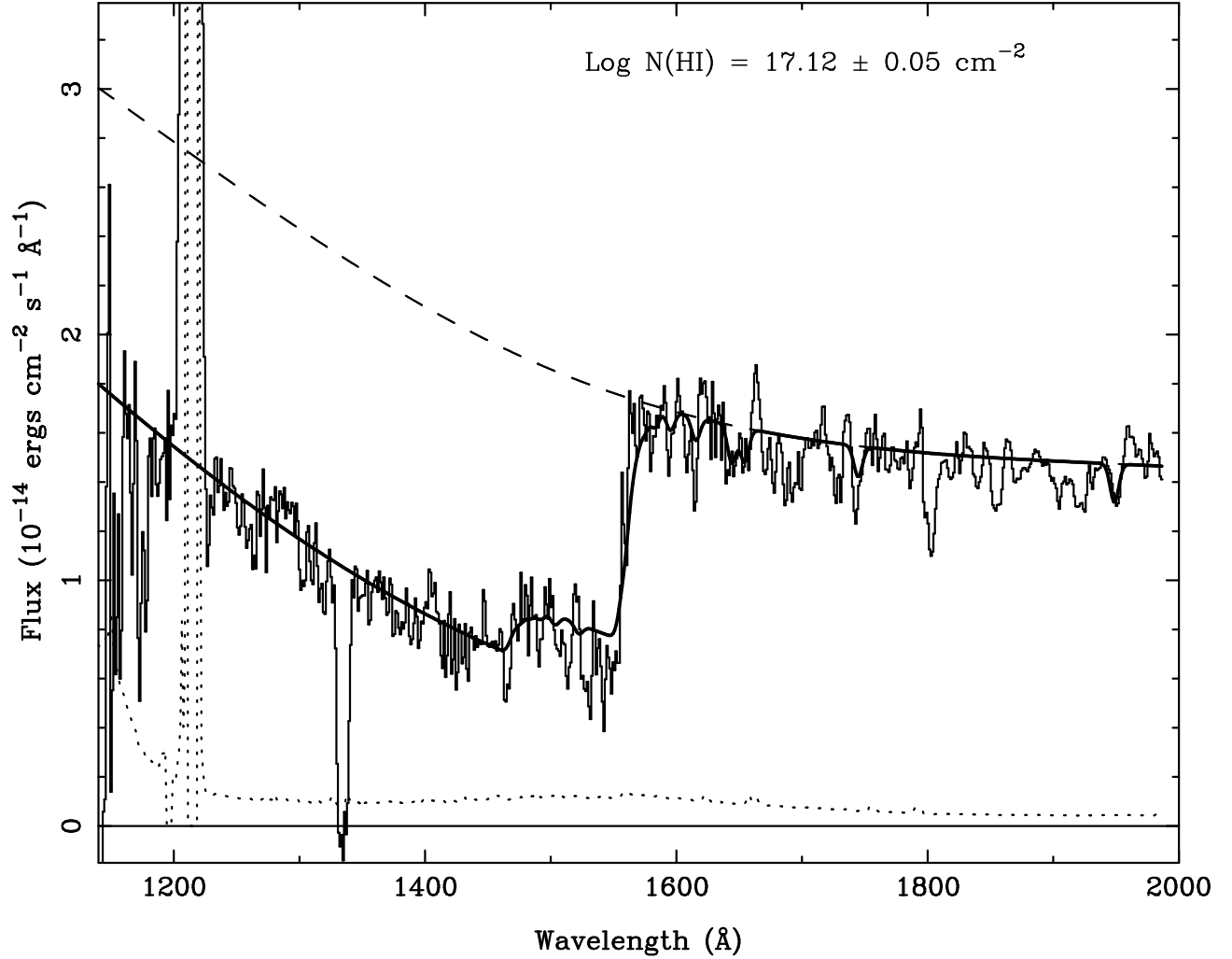


Fig. 3.— IUE spectrum of QSO 1718+4807 ($z_{em} = 1.084$, $V=15.3$). The Lyman limit arising in the system at $z = 0.7011$ is clearly seen as a continuum break near 1550 \AA . The solid line represents hydrogen absorption with $N(\text{H I}) = 17.12$ at this redshift and $N(\text{H I}) = 16.7$ at $z = 0.602$. The dotted line shows the 1σ error array, and the dashed line represents the assumed quasar continuum.

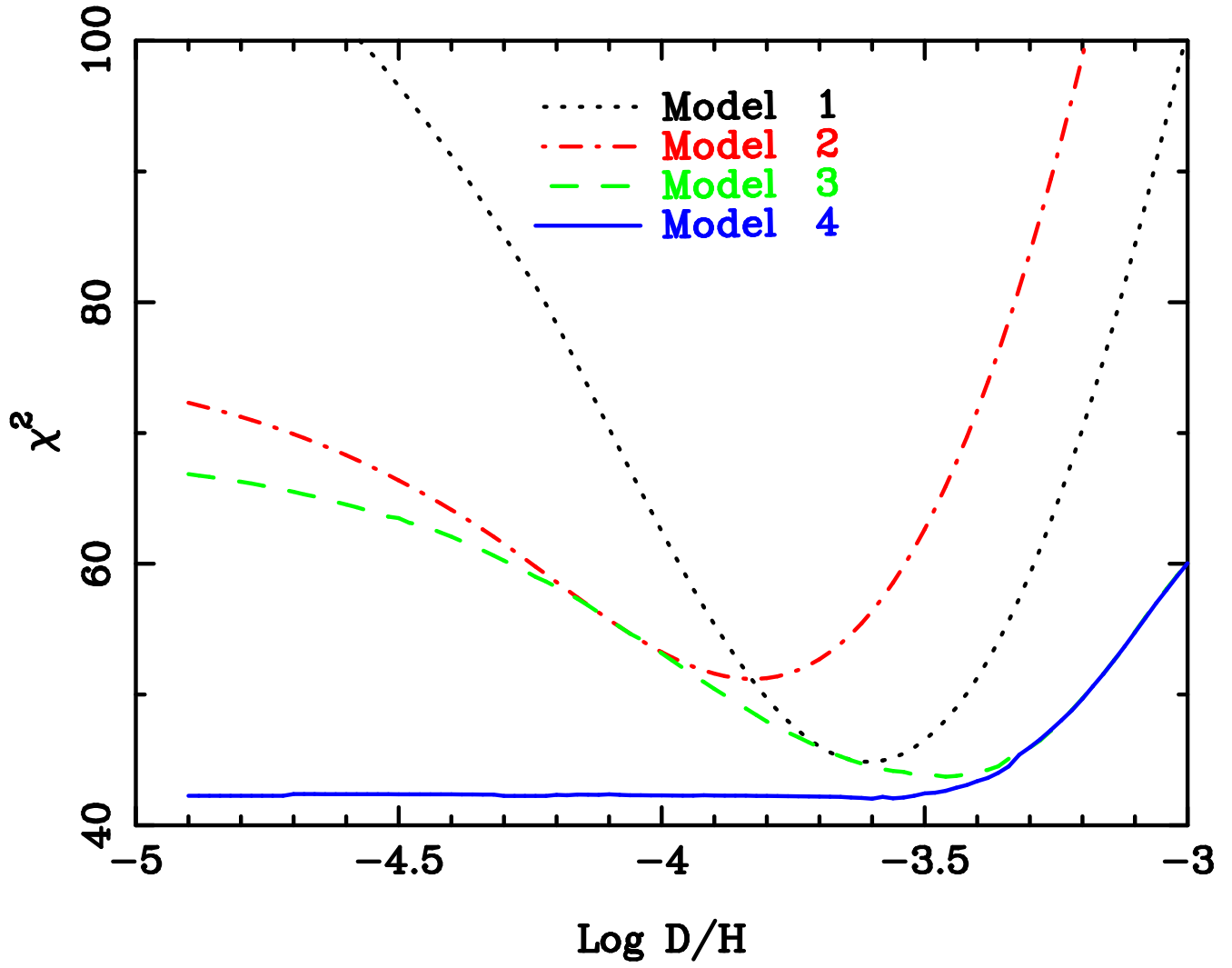


Fig. 4.— χ^2 as a function of D/H for the 4 models.